# A surrogate model for fragility analysis of unanchored storage tanks in seismic prone-areas based on Gaussian process modelling

Hoang Nam Phan[a,b], Fabrizio Paolacci[a]
[a] *Department of Engineering, Roma Tre University, Via Vito Volterre 62, 00146 Rome, Italy*
[b] *The University of Danang – University of Science and Technology, 54 Nguyen Luong Bang street, Da Nang, Vietnam*

*Keywords: Surrogate model; fragility curve; unanchored storage tank; Gaussian process model; Kriging model*

ABSTRACT
An efficient framework for the seismic fragility evaluation of a case study of unanchored steel storage tank is presented in this paper. The framework is based on a surrogate model of the tank that allows using a few simulations of the tank model and hence significantly reduces the computational cost. Firstly, a proper design of experiments approach is selected to generate model samples with input random variables. In particular, the peak ground acceleration and the liquid level are considered as random variables in this study. Three-dimensional finite element models are then built for the generated samples, and nonlinear dynamic analyses are performed using a set of ground motion records. The Gaussian process modelling, also known as Kriging modelling, is finally used to interpolate model responses obtained from the analyses. Since the Kriging model is built, seismic fragility curves of critical failure modes of the tank are derived using Monte Carlo simulations.

## 1 INTRODUCTION

In the framework of the probabilistic seismic risk assessment, the seismic vulnerability evaluation of structures represented by fragility curves has been a key role and indispensable. Although there are some available fragility databases, e.g., for storage tanks, ALA (2001), HAZUS (2001), they are empirically built for general types of structures with the substantial amount of assumptions and uncertainties. Analytical fragility curves are widely used in recent decades. The curves are frequently developed based on results of nonlinear dynamic analyses of structural models. Therefore, the accuracy of fragility functions strongly depends on the reliability of numerical models.

Development of numerical models of storage tanks for modelling the seismic response as well as the damage distribution has received more attention in recent decades. Due to the complexity of various nonlinear mechanisms, three-dimensional finite element (3D FE) models are more suitable in predicting nonlinear response of the tanks. For example, in the case of unanchored tanks, simplified models failed to predict local responses of the tanks caused by uplifting and/or sliding phenomena; therefore, 3D FE models considering full interactions between the tank and the liquid as well as the tank and the foundation are used instead. Unfortunately, the computational time required by these models is rather high. Hence, performing the fragility analysis based on such complex models is not viable.

A valid alternative to improve the computational efficiency is the use of a surrogate model or metamodel, which can be defined as a synthetic model family representing the statistical relation between seismic inputs and structural outputs. This model can be built from a few number of response samples generated through accurate numerical models or experimental data (Bhosekar and Ierapetritou 2018).

Different metamodeling approaches are available in the literature, which are either regression or interpolation models, e.g., high-dimensional model representation (HDMR), polynomial regression, artificial neural network (ANN), LASSO regression, Bayesian network, multivariate adaptive regression spline (MARS), radial basis function network (RBFN), support vector regression (SVR), or Kriging, etc. (Forrester et al. 2018).

Among various types of metamodels, Kriging or Gaussian process regression is selected in this study. The basic idea of Kriging is to predict the value of a function at a given point by computing a weighted average of known values of the function in the neighborhood of the point. This approach treats the function of interest as a realization of a Gaussian random process whose parameters are estimated from available inputs and model responses (Rasmussen and Williams 2004).

Some studies concerning the application of surrogate models in the fragility analysis have been realized recently. Surrogate models are built to calibrate the relation between structural responses and uncertain inputs of structural models, including ground motions and modelling parameters. Gidaris et al. (2015) proposed metamodel framework based on a Kriging surrogate model to approximate the mean and standard deviation of seismic demands which are used to analytically evaluate the seismic fragility curve of a benchmark four-story concrete office building. Zhang and Wu (2017) demonstrated the applicability of a Kriging model to the seismic fragility analysis of an elastoplastic single degree of freedom (SDoF) system and a reinforced concrete bridge.

In this paper, a surrogate model based on Kriging is proposed to build seismic fragility curves of an unanchored storage tank case study. The input random variables represented by the liquid level and the peak ground acceleration are considered, and a reliable design of experiments method is used to generate model samples. 3D FE models for the generated samples are then developed using the ABAQUS software, where the interaction between the tank and the liquid is taken into account by the coupled acoustic-structure analysis. A set of ground motion records is selected, and nonlinear time history analyses are later performed. The Kriging model is built based on the output responses and the input random variables. Consequently, component fragility curves of the tank considering different ranges of the liquid level are evaluated by generating a large enough number of samples with the Monte Carlo technique.

This paper is organised as follows. In Section 2, a brief description of the Kriging-based surrogate model is presented. Section 3 describes how the metamodel can be used for the fragility analysis of unanchored storage tanks. The application of the methodology to a case study of unanchored storage tank is presented in Section 4. Section 5 finishes with some conclusions and perspectives.

## 2 DESCRIPTION OF KRIGING-BASED SURROGATE MODEL

In statistics, Kriging or Gaussian process regression is a method of interpolation for which the interpolated values are modeled by a Gaussian process. Kriging has been widely used as surrogate models or metamodels for deterministic computer models. A Kriging model is a generalized linear regression model that accounts for the correlation between the regression model and the observation.

Considering a computer model $y = G(\mathbf{x})$, where $y$ is considered as a scalar and $\mathbf{x}$ is a vector representing $d$ input parameters. Given $n$ design sites $(\mathbf{x}_1, \mathbf{x}_2, \dots, \mathbf{x}_n)^T$, the computer model output values are $(y_1, y_2, \dots, y_n)^T = (G(\mathbf{x}_1), G(\mathbf{x}_2), \dots, G(\mathbf{x}_n))^T$.

The mathematical form of a Kriging model is given as:

$$Y(\mathbf{x}) = \sum_{j=1}^{p} f_j(\mathbf{x})\,\beta_{\mathrm{j}} + Z(\mathbf{x}) = \mathbf{f}^T(\mathbf{x})\boldsymbol{\beta} + Z(\mathbf{x}) \tag{1}$$

where $f_1(\mathbf{x}), f_2(\mathbf{x}), \dots, f_p(\mathbf{x})$ are known regression functions, $\boldsymbol{\beta} = (\beta_1, \beta_2, \dots, \beta_p)^T$ is a vector of unknown regression coefficients, and $Z(\mathbf{x})$ is a stationary Gaussian random process with zero mean and covariance:

$$\operatorname{cov}\left(Z(\mathbf{x}_{\mathrm{i}}), Z(\mathbf{x}_{\mathrm{j}})\right) = \sigma^2 R\left(\mathbf{x}_{\mathrm{i}} - \mathbf{x}_{\mathrm{j}} | \boldsymbol{\theta}\right) \tag{2}$$

where $\sigma^2$ is the process variance. The spatial correlation function $R\left(\mathbf{x}_{\mathrm{i}} - \mathbf{x}_{\mathrm{j}} | \boldsymbol{\theta}\right)$ with known or unknown correlation parameters $\boldsymbol{\theta}$ controls the smoothness of the resulting Kriging model and the influence of nearby points.

Given the design sites $(\mathbf{x}_1, \mathbf{x}_2, \dots, \mathbf{x}_n)^T$ and corresponding output values $\mathbf{Y}^n = (y_1, y_2, \dots, y_n)^T$, the output values $\mathrm{Y}(\mathbf{x}_0)$ at a new input location $\mathbf{x}_0$ can be predicted using the Kriging model. Assuming that the hyperparameters $\boldsymbol{\theta}$ are known, we have, conditional on $(\boldsymbol{\beta}, \sigma^2)$:

$$\binom{Y(\mathbf{x}_0)}{\mathbf{Y}^n} \sim N_{n+1}\left(\binom{f_0^T}{\mathbf{F}}\boldsymbol{\beta}, \sigma^2\begin{pmatrix} 1 & r_0^T \\ r_0 & \mathbf{R} \end{pmatrix}\right) \tag{3}$$

where $\mathbf{f}_0 = f(\mathbf{x}_0)$ is the $p \times 1$ vector of regression functions of $Y(\mathbf{x}_0)$, $\mathbf{F} = f_j(\mathbf{x}_i)$ is the $n \times p$ matrix of regression functions for the training data, $r_0$ is the $n \times 1$ vector of correlation of $\mathbf{Y}^n$ with $Y(\mathbf{x}_0)$, $\mathbf{R}$ is the $n \times n$ matrix of correlation among the $\mathbf{Y}^n$.

Then, the best linear unbiased predictor (BLUP) of $Y(\mathbf{x}_0)$ is:

$$\hat{Y}(\mathbf{x}_0) = (\mathbf{f}_0^T (\mathbf{F}^T\mathbf{R}^{-1}\mathbf{F})^{-1}\mathbf{F}^T\mathbf{R}^{-1} + \mathbf{r}_0^T\mathbf{R}^{-1}(\mathbf{I}_n - \mathbf{F}(\mathbf{F}^T\mathbf{R}^{-1}\mathbf{F})^{-1}\mathbf{F}^T\mathbf{R}^{-1}))\mathbf{Y}^n \tag{4}$$

The variance of the estimate $\hat{Y}(\mathbf{x}_0)$ is:

$$\mathrm{MSE}\big(\hat{Y}(\mathbf{x}_0)\big) = \sigma^2(1 - \mathbf{r}_0^T\mathbf{R}^{-1}\mathbf{r}_0 + (\mathbf{F}^{\mathrm{T}}\mathbf{R}^{-1}\mathbf{r}_0 - \mathbf{f}_0)^T(\mathbf{F}^T\mathbf{R}^{-1}\mathbf{F})^{-1}(\mathbf{F}^{\mathrm{T}}\mathbf{R}^{-1}\mathbf{r}_0 - \mathbf{f}_0)) \tag{5}$$

In order to obtain a Kriging metamodel, usually, the hyperparameters $\boldsymbol{\theta}$ are unknown and need to be estimated. The maximum likelihood estimation is used in this study. The idea is to find the set of parameters $\boldsymbol{\beta}$, $\sigma_2$, $\boldsymbol{\theta}$ such that the likelihood of the observations $\mathbf{Y}^n$ is maximal.

# 3 FRAGILITY EVALUATION BASED ON SURROGATE MODEL

The first step of the fragility evaluation of unanchored storage tanks based on the surrogate model is the definition of input variables. In the case of storage tanks, the uncertainties in modelling parameters including geometry and material properties are commonly considered. Phan et al. (2019) presented a screening study to find which modelling parameters have significant effects on the seismic response of unanchored tanks. The authors found that the liquid level is the most significant one. Fragility curves considering only the randomness of significant parameters are almost the same with ones considering all modelling parameters. Therefore, in the next section, only the liquid level is considered as the structural random variable to reduce the number of simulations. The randomness of ground motions in terms of the frequency content is also taken into account, where each ground motion is scaled with different $PGA$ values which are randomly generated along with the liquid level.

The second step is to generate samples of input random variables using a proper DOE approach. Among different sampling methods available in the literature, Latin Hypercube Sampling (LHS) is often suggested for Kriging models (Jack and Kleijnen 2017). However, when few random variables are considered, Central Composite Design (CCD) also represents a valid alternative (Paolacci and Giannini 2009). This sampling method is widely used in response surface applications. By selecting corner, axial, and center points, it is an ideal solution for fitting a second-order response surface model. However, as it requires a relatively large number of sample points, the CCD method should only be chosen when the total number of significant variables is reduced.

In the third step, the 3D FE model is developed for each sample, and the nonlinear time history dynamic analysis is performed on each structure-earthquake pair. The peak responses are measured at each analysed ground motion. The mean and standard deviation of the measured responses are calculated assuming a lognormal distribution. Hence, two experiment designs will be obtained, one for the mean value of the measured responses and the other one for their standard deviation.

The fourth step is the development of the Kriging model for the mean and standard deviation of the responses. One the Kriging modes are built, a composed Kriging model is developed:

$$\hat{\mathbf{Y}} = e^{\hat{\mathbf{Y}}_\mu + LogN(0,\hat{\mathbf{Y}}_\sigma)} \tag{6}$$

where, $\hat{\mathbf{Y}}_\mu$ and $\hat{\mathbf{Y}}_\sigma$ are, respectively, the Kriging model of the mean and standard deviation of the response quantity. Equation (11) supposes a lognormal distribution of the response. The Monte Carlo simulations can be carried out based on the composed Kriging model by sampling the input random variables. Once a large enough number of predicted response values at a given $PGA$ are obtained, the empirical fragility curve, which presents the probability of exceeding a given limit state, can be derived.

# 4 APPLICATION TO CASE STUDY

## *4.1 Description of case study*

An existing tank ideally installed in a refinery in Sicily (Italy), which well represents a broad geometry, is selected for this study. The tank is a 54.8-m-diameter cylindrical steel tank and unanchored with respect to the foundation. The tank height is 15.6 m, and the capacity of the tank is 37044 $\mathrm{m}^3$. The tank is provided with a floating roof; however, the effect of the floating roof is neglected in this study. The shell thickness has been designed varying from 8 mm at the top course to 33 mm at the bottom course. The bottom plate has a uniform thickness of 8 mm. The tank is assumed to fill with water at a filling level of 14 m (i.e., 90% of the tank height). Both shell and bottom plate are structured by S235 carbon structural steel having a yield strength of 235 MPa. More detail of nominal material and geometry properties is illustrated **Errore. L'origine riferimento non è stata trovata.**.

Table 1. Nominal material and geometry properties of the tank.

| | Property | Design value |
|---|---|---|
| Tank | Density (kg/m$^3$) | 7850 |
| | Young's modulus (MPa) | 200000 |
| | Poisson's ratio | 0.3 |
| | Yield strength (MPa) | 235 |
| | Radius of tank (m) | 27.432 |
| | Height of tank (m) | 15.6 |
| | Shell plate thickness (mm) | 33, 29.5, 25.5, 21.5, 17.5, 14, 10, 8, 8 |
| | Bottom plate thickness (mm) | 8 |
| Liquid | Density (kg/m$^3$) | 998.21 |
| | Liquid level (m) | 14 |

## *4.2 Input parameters and design sites*

In this study, the randomness in the filling level of the contained liquid and the ground motion is considered. The filling level has been demonstrated as the most significant parameter that affects the seismic vulnerability of unanchored tanks (Phan et al. 2019). A variation of the filling level from 50% to 100% (i.e., 7 to 14 m) of the maximum level is assumed, which follows a uniform distribution, while $PGA$ follows a lognormal distribution with a mean of 0.6 g and a variation in logarithmic scale of 0.2. The lower and upper bounds of $PGA$ are calculated as:

$$PGA_{-}^{+} = e^{ln0.6 \pm 0.2} = \begin{matrix} 0.8 \text{ g} \\ 0.45 \text{ g} \end{matrix} \quad (7)$$

The input random variables are summarized in Table 1.

Table 2. Random variables considered in the model.

| Variable | Distribution | Parameters | |
|---|---|---|---|
| $H$ (m) | Uniform | $L$ = 7 m | $U$ = 14 m |
| $PGA$ (g) | Lognormal | $m$ = 0.6 g | $v$ = 0.2 |

The CCD method is used to generate samples of the random variables. It is composed of $2^n$ points of the full factorial two-level design, with all the variables at their extremes, plus a number of repetitions of the nominal design, plus $2n$ points obtained by changing one design variable at a time by an amount $\alpha$. The value of $\alpha$ depends on the number of experimental runs in the factorial portion of the CCD. For two random variables presented in Table 2, 9 samples will be obtained assuming only one center point. Figures 2 shows the CCD for $n = 2$, where $\alpha = 2^{2/4} = 1.41$. The CCD table is shown in Table 3, where the corresponding values of $H$ and $PGA$ for each sample are also calculated.

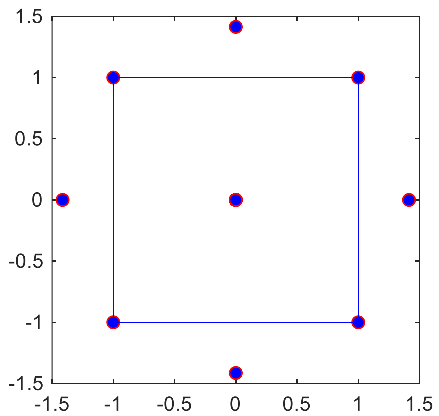


Figure 1. Central composite design.

Table 3. Central composite design table.

| N. samples | Factors | | Calculated real values | |
|---|---|---|---|---|
| | $X_1$ | $X_2$ | $H$ (m) | $PGA$ (m) |
| 1 | -1 | -1 | 7.0 | 0.49 |
| 2 | -1 | 1 | 7.0 | 0.73 |
| 3 | 1 | -1 | 14.0 | 0.49 |
| 4 | 1 | 1 | 14.0 | 0.73 |
| 5 | -1.41 | 0 | 5.6 | 0.60 |
| 6 | 1.41 | 0 | 15.4 | 0.60 |
| 7 | 0 | -1.41 | 10.5 | 0.45 |
| 8 | 0 | 1.41 | 10.5 | 0.80 |
| 9 | 0 | 0 | 10.5 | 0.60 |

## *4.3 3D FE modelling*

The tank-liquid system subjected to earthquake loadings is modelled using the FE analysis package ABAQUS (SIMULIA 2014). The coupled acoustic-structural analysis, which was presented and validated by Phan and Paolacci (2018), is used in this study. This approach is simple and effective to treat numerically, as it assumes no material flow and thus no mesh distortion. The FE meshes of steel tank consist of four-node, doubly curved quadrilateral shell elements (S4R). Each node of shell element has three translational and three rotational degrees of freedom. The liquid is modelled using eight-node brick acoustic elements (AC3D8). The acoustic FE model is based on the linear wave theory and considers the dilatational motion of the liquid. To derive the equations for acoustic wave propagation, a number of assumptions have to be made to simplify the equations of fluid dynamics.

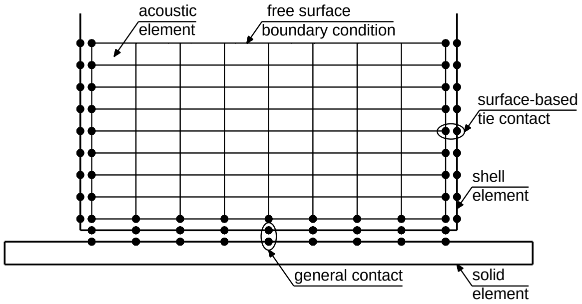

Figure 2. Boundary conditions of the liquid-tank model.

The tank-liquid interaction is considered using a surface-based tie constraint between the tank inner and liquid surface. This constraint is formulated based on a master-slave contact method, in which normal force is transmitted using tied normal contact between both surfaces through the simulation. The sloshing waves are considered in the liquid model assuming small-amplitude gravity waves on the liquid free surface.

The bottom plate of the tank is unanchored and rested on a rigid slab that is modelled using solid elements. The successive contact and separation between the tank bottom plate and its rigid foundation are taken into account by a surface-based contact modelling algorithm. The boundary conditions of the model are shown in Figure 2.

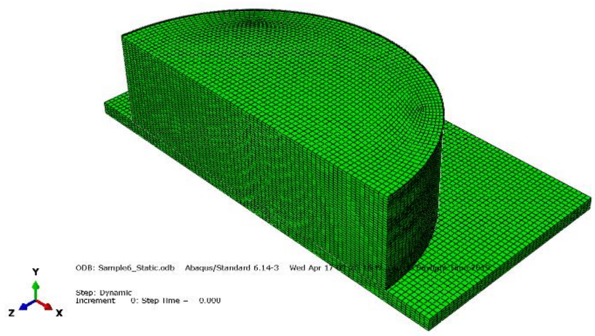
Figure 3. Numerical model of the tank-liquid system.

Both geometric and material nonlinearities are considered in the analysis. The plasticity of the steel tank is modelled based on the stress-strain curve of the material. The curve obtained from mechanical testing is converted into true stress and the plastic strain. The water density is considered to be 998.21 kg/m$^3$, and its bulk modulus is 2150 MPa. The Rayleigh mass proportional damping is employed for the tank model assuming a damping ratio of 2.0%, for the fundamental vibration mode of the tank-liquid system. Due to the structural symmetry and to reduce the computational cost, only half of the tank-liquid system is modelled, and symmetry plane boundary conditions are employed. The mesh convergence analysis results in an optimal mesh size of 0.4 m and 0.8 m in the longitudinal direction and the circumferential direction, respectively, to achieve acceptable accuracy. The mesh near the shell-to-bottom joint is a fine mesh of 0.1 m in the longitudinal direction. An example of the FE mesh of the Sample 6 model is illustrated in Figure 3.

### 4.4 *Static pushover analyses*

The most severe case, i.e., Sample 6 with the highest level of the liquid, is selected for the pushover analysis. The aim of the analysis is to primarily evaluate the static behaviour of the tank. For the development of a static pushover model, the acoustic elements are ignored, and a pushover loading is used instead. Three loading steps are applied as shown in Figure 4, where the hydrodynamic load is calculated using the formula in the Eurocode 8 (EN1998-4 2006).

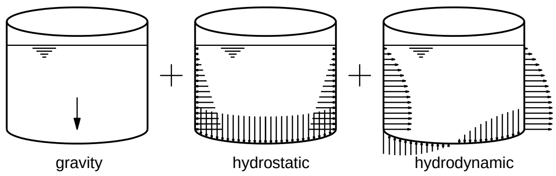

Figure 4. Loading steps of the pushover analyses

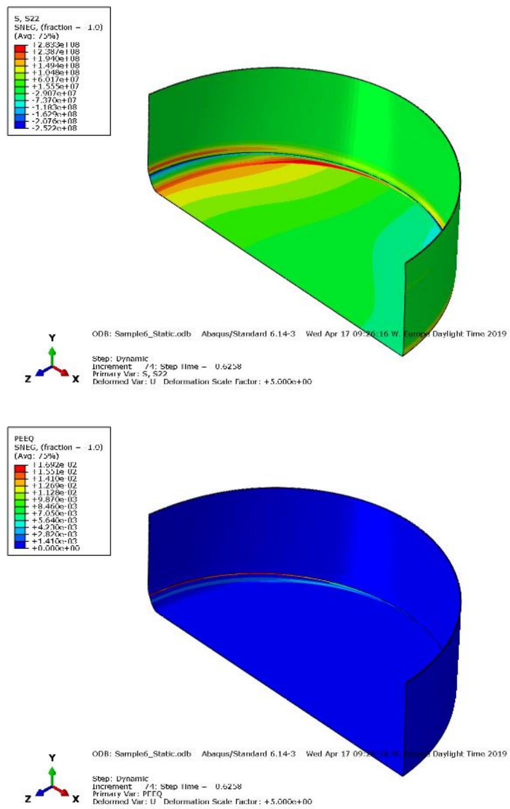
Figure 5. Von Mises stress contour at the last time step of the analysis.

The hydrodynamic pressure acting on the tank shell and bottom plate is increased with the increase of the ground acceleration until an acceleration level around 0.63 g. At this point, the numerical instability occurs that is due to the failure of the shell-to-bottom connection.

Static responses in terms of the uplift displacement of the bottom edge, the compressive and hoop stresses of the shell plate, the Von Mises stress, and the equivalent plastic strain of the shell plate and shell-to-bottom connection are observed for the shell plate and the shell-to-bottom connection as shown in Table 4. An example of the Von Mises stress contour is shown in Figure 5.

Table 4. Observed equivalent plastic strain at a ground acceleration level of 0.63 g.

| Quantity | Shell plate | Shell-to-bottom connection |
|---|---|---|
| Uplift displacement (m) | - | 0.51 |
| Compressive meridional stress (MPa) | 22.5 | - |
| Hoop stress (MPa) | 225 | - |
| Von Mises stress (MPa) | 222 MPa | 292 MPa |
| Equivalent plastic strain | $6.2 \times 10^{-4}$ | $1.7 \times 10^{-2}$ |

It can be seen that the shell-to-bottom connection almost reaches the ultimate point while the shell plate is still in the elastic range; this demonstrates the vulnerability of the shell-to-bottom connection in unanchored tank structures. The stress level in the connection significantly increases due to the uplift of the bottom plate.

Although a high level of the uplift displacement is observed, the buckling of the shell plate is not visible. A small value of the compressive meridional stress in the shell plate is observed while the hoop stress reaches almost the yielding point, as illustrated in Table 4.

The nonlinear static pushover results explicate that the most critical failure mode of the tank is the failure of the connection. The occurrence of the shell plate failure due to the material yielding and the shell plate buckling is rather limited.

In the following, only two critical failure modes are considered, i.e., the fracture of the connection caused by the rotation demand and the material yielding of the shell plate caused by the hoop stress.

### 4.5 *Selection of ground motion records for nonlinear time history analyses*

With the aim to demonstrate the capability of the method in reducing significantly the number of simulations, only eight records are selected and used for dynamic time history analyses of the 3D FE model. The tank is supposed to be ideally placed in one of the most seismically active zones in Sicily (Italy), just close to Priolo Gragallo city, characterized by soil type B. The records are selected for a return period of 2475 years and based on a uniform hazard spectrum (solid red line in Figure 6) that was obtained from the seismic hazard analysis of the site. The records are selected so that the median response spectrum (solid black line) and median ±σ (16th and 84th percentile) have the best fit to that of the target UHS. The response spectra of the selected records are shown in Figure 6.

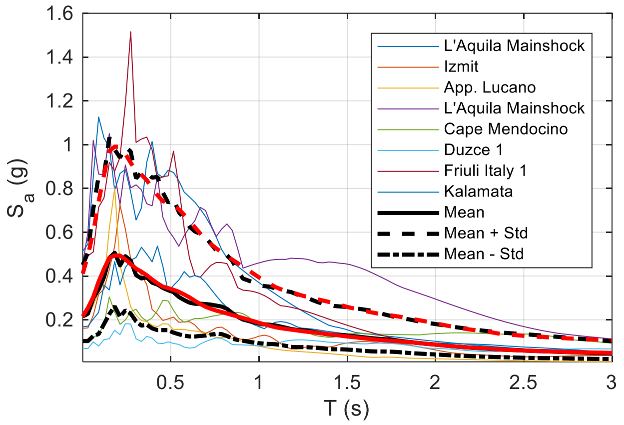


Figure 6. UHS-based record selection.

### 4.6 *Construction of Kriging-based surrogate model using nonlinear time history analysis results*

As the result of the CCD, 9 model samples with different combination of $H$ and $PGA$ are generated. Each sample is modelled using the 3D FE model and subjected to 8 selected records. The records are scaled with respect to the $PGA$ value provided in Table 3. Therefore, 72 simulations are carried out. An example of the Von Mises stress and the equivalent plastic strain contours are shown in Figure 7. The response quantities are measured at $t = 4.06\,s$ from the analysis of Sample 6 subjected to Kalamata earthquake.

It can be seen from the figures that the shell-to-bottom joint reaches the yielding while the shell and bottom plate are still in the elastic region; this agrees well with the observation from the nonlinear static analysis.

The time history data of the uplift response at two ends of the bottom plate is shown in Figure 8. A maximum uplift displacement of 0.5 m is recorded. Similarly, the peak seismic response in terms of the uplift displacement is measured for all the samples. The corresponding rotation demand of the joint is then calculated that is a function of the uplift displacement, the uplift length, and the radius of the tank (EN 1998-4 2006). The hoop stress of the shell plate is also measured for each sample analysis. The stress is calculated as the maximum value among those obtained from all shell courses. The results in terms of the rotation demand of the shell-to-bottom connection and the hoop stress of the shell plate are plotted in Figure 9. It can be seen that Sample 4 and 6 exhibit high seismic demands due to the high level of the liquid; whereas, the responses obtained from Sample 1 and 5 are rather small.

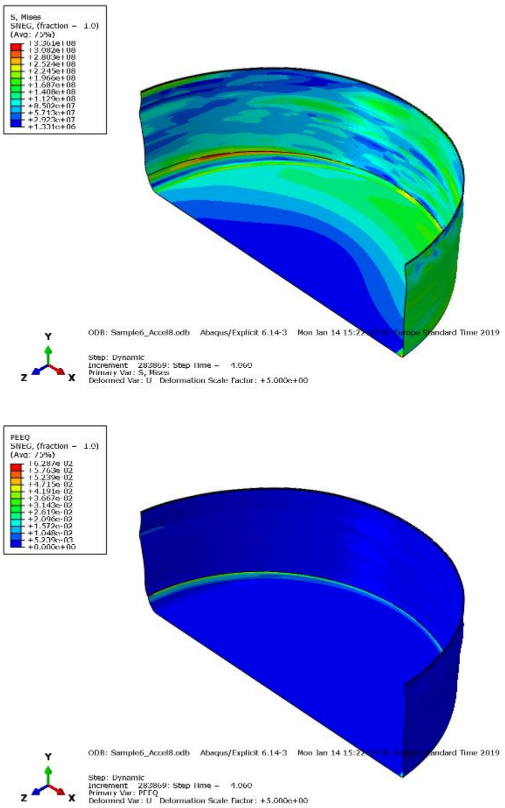

Figure 7. Example of numerical results in terms of Von Mises stress and equivalent plastic strain contours (Sample 6, Kalamata earthquake, t = 4.06 s).

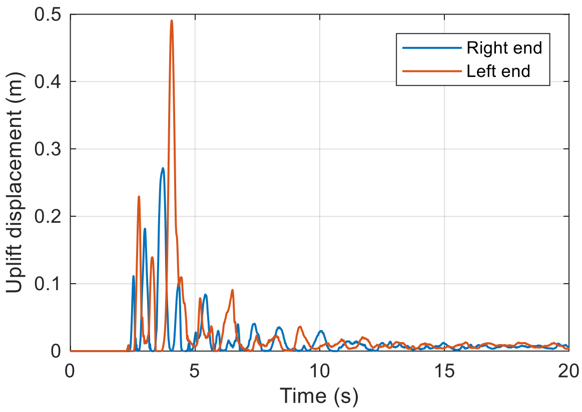


Figure 8. Time history data of uplift at the left and right ends of the bottom plate (Sample 6, Kalamata earthquake).

The analyses consider the uncertainty of the ground motions in terms of $PGA$. At each $PGA$ value, the responses vary due to the effect of the frequency content from different ground motions. Therefore, the transient analysis results are not able to use as an input in the above Kriging model. The mean and standard deviation values of the response are used instead.

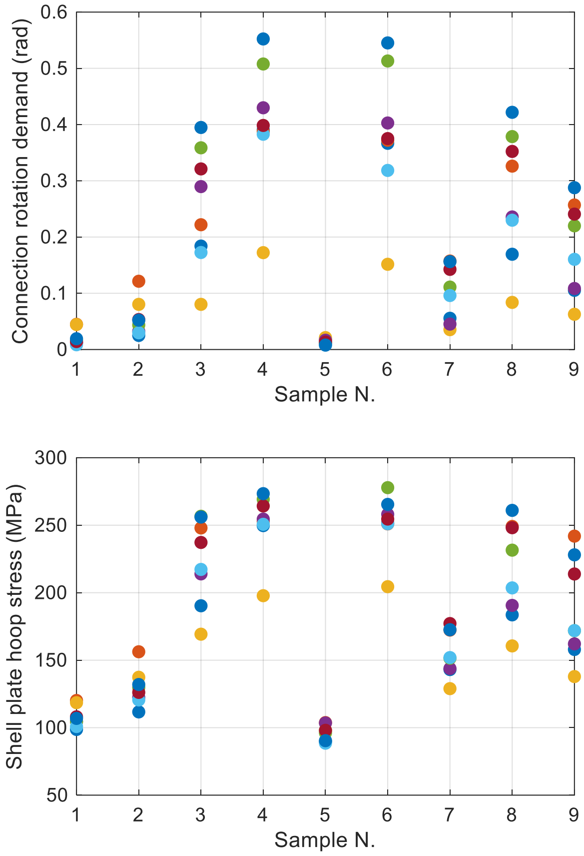


Figure 9. Model outputs in terms of the rotation demand of the connection and the hoop stress demand of the shell plate.

Kriging models are built for the mean and standard deviation of the responses using the UQLAB software (Lataniotis et al. 2018), in which the linear function is used as the basic function of the model. The correlation type is given by the separable correlation function, and the correlation family is given by the Matern 3/2 kernel function. The hyperparameters are assessed using the maximum likelihood estimation. The genetic algorithm is adopted to solve the global optimization of the model.

Once the two Kriging models are built, the composed Kriging model is then obtained by using Equation (6) that is assumed to follow a lognormal distribution.

### 4.7 *Fragility analysis*

The failure of the weld between the bottom plate and the shell due to the rotation of the plastic hinge is considered. A limit of 0.2 rad is assumed for the hinge rotation based on a maximum allowable strain of 0.05 (EN 1998-4 2006). On the other hand, the stress limit of the material yielding of the shell plate is $0.9\sigma_y$, where $\sigma_y$ is the yielding strength of the steel.

Given the limit states, the fragility curves of the corresponding failure modes are developed using Monte Carlo simulations that can be carried out based on the composed Kriging model in Equation (11). The simulations are repeated for each specific $PGA$ value, for example, in this study, a range of $PGA$ varying from 0.005 g to 1.2 g with a step size of 0.005 g is considered. The data post-processing on the 100000 observations leads to fragility curves of the two failure modes in Figure 10. To obtain a smooth curve, a large sample set must be used; this is only possible when a surrogate model is used.

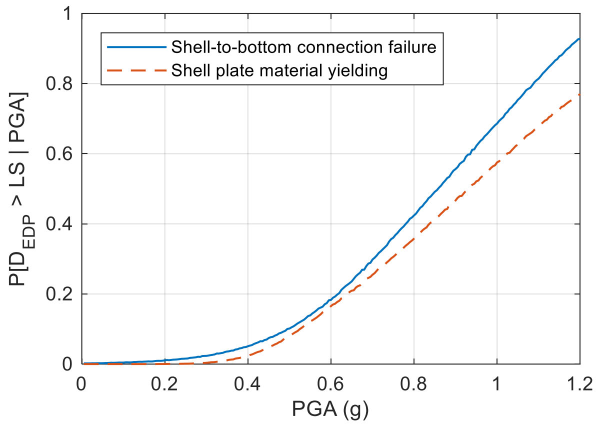


Figure 10. Fragility curves of the shell-to-bottom connection failure and the shell plate material yielding

The fragility curves presented in Figure 10 show the probabilities of exceeding the rotation limit of the plastic high at the connection and the yielding stress limit of the shell plate. The occurrence probability of the connection failure is slightly higher than one of the shell plate yielding.

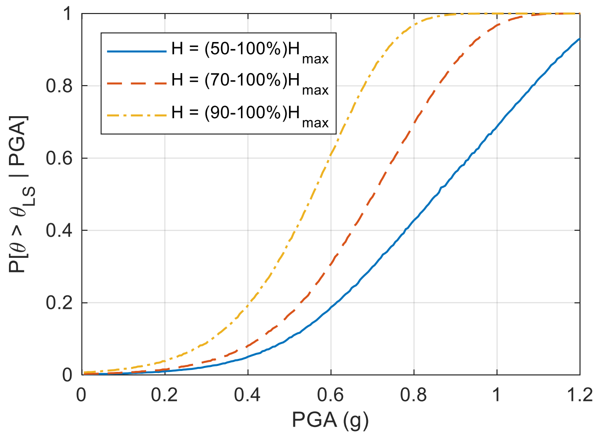


Figure 11. Fragility curve of the shell-to-bottom joint failure considering different ranges of the liquid level.

The capability of the surrogate model is also demonstrated with quickly building fragility curves for different ranges of the inputs. For example, Figure 11 shows fragility curves of the shell-to-bottom connection failure for three different ranges of the liquid level. This is not possible in traditional approaches, where a large number of analyses need to run again.

## 5 CONCLUSIONS

In this paper, a framework of the seismic fragility evaluation of aboveground unanchored tanks using the Kriging-based surrogate model is presented. The surrogate model is developed based on a proper design of experiment approach and a 3D FE model of the tank. Due to the high computational cost of refined model simulations, the current procedure relies on a limited number of dynamic analyses. The Kriging-based surrogate model allows for the computation of responses to numerous samples of input variables without running new finite element analyses. The application to a case study of the unanchored tank demonstrates the capability of the present procedure of obtaining fragility curves for different input conditions.

## ACKNOWLEDGMENTS


The work presented herein was partially carried out with a financial grant from the research fund for the European Commission, within the research project SERA (Grant No. 730900).


## REFERENCES


ALA, 2001, Seismic fragility formulation for water system: Part 1-Guideline, ASCE.

Bhosekar T., Ierapetritou M., 2018, Advances in surrogate based modeling, feasibility analysis, and optimization: A review, *Computers & Chemical Engineering*, Vol 108, pp 250-267.

EN 1998-4, 2006, Eurocode 8: Design of structures for earthquake resistance - Part 4: Silos, tanks and pipeline, Brussels, Belgium.

Forrester A.I.J., Sóbester A., Ke A.J., 2008, Engineering Design via Surrogate Modelling: A Practical Guide, John Wiley and Sons, Ltd.

Gidaris, I., Taflanidis, A.A., and Mavroeidis, G.P., 2015, Kriging metamodeling in seismic risk assessment based on stochastic ground motion models, *Earthquake Engineering & Structural Dynamics*, Vol. 44, No. 14, pp. 2377-2399.

HAZUS, 2001, Earthquake loss estimation methodology, National Institute of Building Science, Risk Management Solution, Menlo Park, CA, USA.

Jack P.C., Kleijnen, 2017, Regression and Kriging metamodels with their experimental designs in simulation: A review, *European Journal of Operational Research*, Vol. 256, No. 1, pp. 1-16.

Lataniotis, C., Marelli, S., Sudret, B., 2018, UQLab user manual – Kriging (Gaussian process modelling), Report

UQLab-V1.1-105, Chair of Risk, Safety & Uncertainty Quantification, ETH Zurich.

Phan, H.N., Paolacci, F., 2018, Fluid-structure interaction problems: An application to anchored and unanchored steel storage tanks subjected to seismic loadings, Proceedings of the 16th European Conference on Earthquake Engineering (16ECEE), Thessaloniki, Greece.

Phan H.N., Paolacci F., Alessandri S., 2019, Enhanced Seismic Fragility Analysis of Unanchored Steel Storage Tanks Accounting for Uncertain Modeling Parameters, *Journal of Pressure Vessel Technology*, Vol. 141. No. 1, pp. 010903-010903-10.

Paolacci F., Giannini R., 2009, Seismic reliability assessment of a disconnect switch using an effective fragility analysis, *Journal of Earthquake Engineering*, Vol. 13, pp. 217-235.

Rasmussen, C.E., Williams, C.K.I., 2006, Gaussian processes for machine learning, The MIT Press.

SIMULIA, 2014, Abaqus 6.14 Documentation, Dassault Systèmes Simulia Corp., Providence, RI, USA.

Zhang, Y., Wu, G., 2017, Seismic Vulnerability Analysis of RC Bridges Based on Kriging Model, *Journal of Earthquake Engineering*, Vol. 23, No. 2, pp. 242-260.